Agricultural and Forest Meteorology 376 (2026) 110924

Contents lists available at ScienceDirect

Agricultural and Forest Meteorology

journal homepage: www.elsevier.com/locate/agrformet

Greater increase in surface albedo following clear-cutting than wildfire in pine dominated northern Swedish boreal forests

Eirik Næsset Ramtvedt [a,*], Ryan M. Bright [b], Terje Gobakken [a], Adrián Cidre-González [a,c], Maja K. Sundqvist [d], Zsofia R. Stangl [d], Marie-Charlotte Nilsson [d], Daniel B. Metcalfe [e], Michael J. Gundale [d]

[a] Norwegian University of Life Sciences, Faculty of Environmental Sciences and Natural Resource Management, 1432 Ås 5003, Norway
[b] Norwegian Institute of Bioeconomy Research, 1431 Ås 115, Norway
[c] University of Cordoba, Department of Forest Engineering, Campus de Rabanales, Cordoba 14071, Spain
[d] Swedish University of Agricultural Sciences, Department of Forest Ecology and Management, Umeå SE901-83, Sweden
[e] Umeå University, Department of Ecology and Environmental Science, Umeå SE901-87, Sweden

ARTICLE INFO

Keywords:
Surface albedo
Satellite remote sensing
Boreal forest
Forest management
Unmanaged forests

ABSTRACT

There is a public debate on how boreal forests can deliver climate change mitigation benefits. While most debates regarding Fennoscandian forests have centered on the contrasting effects of actively managed and old-growth unmanaged forests on carbon uptake and storage, the impact of surface albedo has often been overlooked. According to the new EU forest strategy for 2030, with aim of improving quantity and quality of forests by promoting primary old-growth forests and avoiding clear-cutting, among others, we examined how albedo across a wide age range of boreal *Pinus*-dominated forests develops over time after wildfire (defined as unmanaged) and clear-cutting (defined as managed). We find that albedo decreases over time after disturbance, but mainly in managed forests. Annual mean albedo in young (<30 years) managed forests (0.36±0.04) is markedly larger than in young unmanaged forests (0.18±0.04). This difference is particularly prominent during winter, when snow-covered ground is present. The mean albedo over the entire unmanaged forest-age gradient (0.17±0.05) is significantly lower ($p < 0.05$) than that of the managed forest-age gradient (0.23±0.10). Considering the typically higher frequency of clear-cuts compared to wildfires in Fennoscandian forests, these albedo differences would be even larger over long time scales. Our findings reveal the importance of considering the climatic cooling potential of albedo when making decisions on how to optimize future forest management in northern boreal forests to mitigate climate change.

1. Introduction

Boreal forests play a critical role in the global carbon cycle by sequestering large amounts of CO_2 from the atmosphere through photosynthesis and storing carbon in soils (Bonan, 2008; Bradshaw and Warkentin, 2015; Nabuurs et al., 2013). By adopting the Kyoto Protocol in 1997, the role of forests and forestry was highlighted for the first time as a means to sequester a portion of the growing emissions of greenhouse gases. Today, there is strong pressure for boreal forest management practices to optimize the delivery of a multitude of ecosystem services – including biomass production, biodiversity, and climate regulation (Eyvindson et al., 2018; Lindahl et al., 2017; Pohjanmies et al., 2017) – to fulfill the goals set by the Paris Agreement on climate change and the Kunming-Montreal Global Biodiversity Framework. As part of these climate-related forest policies, the climate benefits associated with primary unmanaged boreal forests versus even-aged managed forest stands (i.e., where trees are of similar age) have become increasingly discussed. For instance, forest-related land use change in Sweden, largely driven by the expansion of rotational forestry, i.e., where forests are clear-cut, planted, thinned, and eventual cut again (Ahlström et al., 2022), has sparked contrasting viewpoints regarding its impact on climate. Proponents of rotational forestry argue that younger managed forests serve as stronger carbon sinks because of their higher rates of net primary production relative to older stands (Tang et al., 2014). Conversely, others emphasize the importance of old-growth unmanaged forests, which store larger quantities of carbon in both biomass and soil over

* Corresponding author.
E-mail address: eirik.nasset.ramtvedt@nmbu.no (E.N. Ramtvedt).

https://doi.org/10.1016/j.agrformet.2025.110924
Received 7 February 2025; Received in revised form 26 October 2025; Accepted 3 November 2025
Available online 11 November 2025

long periods, thereby reducing atmospheric CO_2 concentrations (Bradshaw et al., 2009; Luyssaert et al., 2008). Despite this ongoing discussion, the climate effect derived from altered albedo during these forest transitions has been almost entirely overlooked.

Surface albedo, the fraction of incoming solar radiation reflected by the land surface, is a key parameter governing Earth's energy balance (Wang et al., 2019). Over the last decade, we have acquired an increased understanding of how forest management practices impact albedo. These practices are mainly related to alterations of stand age and forest structural- and species compositions (Bright et al., 2013; Kuusinen et al., 2014; 2016). Ignoring the climate effect of albedo can potentially lead to incorrect conclusions about the climate impacts of management in boreal forests (Bright et al., 2014; Hasler et al., 2024). This emphasizes the importance of incorporating albedo as a standard boreal forest service related to climate regulation. However, doing so is not a trivial task, as different studies suggest different climatic outcomes depending on the local climatic and environmental conditions (Bright and Astrup, 2019), the interplay between the opposing effects of albedo and carbon sequestration (Bright et al., 2024; Hovi et al., 2016; Rautiainen et al., 2011; Kellomäki et al., 2021; 2023), and the methods employed to compare the two effects (Bright and Lund, 2021). Therefore, reliable assessments of climate effects from albedo changes linked to forest planning require reliable information at spatial scales aligned with those of local forestry (Bright et al., 2024).

Despite improved knowledge about how forestry impacts albedo, less effort has been made to quantify and understand albedo differences between managed versus unmanaged boreal forests. Acquiring this knowledge is critical for finding an optimal solution maximizing ecosystem services provided by boreal forests. Notably, about 35 % of the global forest area is classified as "old-growth" or "primary" unmanaged forest (FAO, 2015), of which the boreal forest accounts for 50 % (Mackey et al., 2015). Wildfires are a major disturbance in unmanaged boreal forests around the globe and wildfires are becoming more frequent and severe (Flannigan et al., 2013; Jones et al., 2024; Kinnunen et al., 2024). The relevance of albedo to the climate effect of forest fires has been clearly illustrated across different types of boreal forests (O'Halloran et al., 2012; Randerson et al., 2006; Stuenzi and Schaepman-Strub, 2020). Whereas wildfires serve as the dominant stand-replacing natural disturbance agent in boreal North America (Brassard and Chen, 2008; 2010), less intense surface fires are common in Fennoscandia (Finland, Norway, Sweden, Karelia, and Kola Peninsula in Russia) and northwest Eurasia (Rogers et al., 2015). It has been reported that albedo is dependent on fire severity and post-fire successional dynamics (Amiro et al., 2006; O'Halloran et al., 2014; Rogers et al., 2015), with snags potentially being the dominant controller of post-fire albedo on decadal timescales (O'Halloran et al., 2014). Several studies have reported substantial increases in winter and spring albedo for stand-replacing fires in North American forests (Amiro et al., 2006; Lyons et al., 2008; Randerson et al., 2006; Rogers et al., 2015). However, observational studies of post-fire albedo dynamics, particularly over longer time periods, are not available for lower-severity wildfires in unmanaged boreal forests, such as in Fennoscandia.

Apart from two simulation studies that compared carbon and albedo dynamics for an unmanaged and managed spruce forest (Kellomäki et al., 2021; 2023), no study has explicitly compared temporal changes in albedo during stand development for these boreal forest types in Fennoscandia based on observational data, nor have studies assessed the albedo effects of converting managed forests into unmanaged forests. Doing so is highly relevant to enable an assessment of the entire array of climate effects between these two forest types over relevant timescales. In this study, we examined whether albedo differs between post-clear-cutting (defined as managed) and post-wildfire (defined as unmanaged) forests under comparable site conditions during stand development. We established two contrasting forest chronosequences (i.e., forest-age gradients based on space-for-time substitution) in northern Sweden, including an unmanaged and an even-aged managed chronosequence (n = 18, respectively), where wildfire versus clear-cutting served as the disturbance agent, respectively. Monthly high-resolution albedo data were retrieved for each forest stand using a direct estimation approach for Sentinel-2 reflectance imagery (Bright and Ramtvedt, 2024).

2. Material and methods

2.1. Establishment of forest chronosequences

Our study employed two contrasting chronosequences in managed and unmanaged boreal forests (Fig. 1), respectively, in northern Sweden (Västerbotten and Norrbotten County), within an area spanning 190 km north–south and 150 km east–west. Both chronosequences are dominated by Scots pine (*Pinus sylvestris* L.), with rare presence of Norway spruce (*Picea abies* (L.) Karst) and birch (*Betula pubescens* Ehrh.). The chronosequences were established based on 36 selected forest stands evenly divided between the two forest types. We started the stand selection by using a forest inventory database provided by Sveaskog AB (Buness et al., 2025) to identify potential stands as those dominated by *Pinus* with mesic site conditions (i.e., moderate moisture levels). The criterion of mesic site conditions ensured that environmental differences between the stands were as small as possible, by excluding extremely wet or dry forests. Next, we conducted a field survey of candidate unmanaged stands, where inclusion or exclusion was determined based on visual inspection of understory vegetation and verification of fire occurrence. We used understory vegetation consisting of feathermosses (*Hylocomium splendens* and *Pleurozium schreberi*) and specific ericaceous dwarf shrubs (*Vaccinium myrtillus, Vaccinium vitis-idaea*, and *Empetrum nigrum*) as indicators of mesic site conditions, whereas forest stands with understories of wet (*Sphagnum* sp. and *Ledum palustre*) or dry (*Cladonia* sp. and *Calluna vulgaris*) community dominance types were considered non-mesic, and thus excluded. Tree coring was done to estimate the fire year, thereby determining the stand age of the unmanaged stands. For unmanaged stands that met the criteria of mesic vegetation type and historical fire occurrence, we used a GIS framework to locate nearby candidate managed stands. The same understory vegetation criteria applied to unmanaged forest stands were then used to confirm the suitability of potential managed stands. For both managed and unmanaged stands we intentionally selected stands to span as wide a range of time since clear-cutting (for managed stands) and wildfire (for unmanaged stands). This process resulted in two chronosequences: one for 18 managed forests with stand age spanning 1–109 years after clear-cutting, and one for 18 unmanaged forests spanning 4–375 years after fire. Both chronosequences spanned the entire age range typically found in managed and unmanaged forests in northern Sweden. In the managed forest stands, even-aged management has been implemented, including clear-cutting, planting, and typically 2–3 thinning operations. Unavoidably, the management practices used to achieve even-aged forest stands have changed over the past century, and thus observed changes along the managed chronosequence also partly reflect the development of management practices for timber production. A wide range of fire severity has occurred in the unmanaged forest stands, with minimal visible traces of forest management for timber production, except for the oldest unmanaged chronosequence stands (>160 years old), where as much as ca. 10 % of trees were selectively logged at the end of the 1800s and early 1900s (Buness et al., 2025). However, remaining trees have had a long period to compensate for this disturbance, and we consider this effect negligible.

2.2. Tree measurements

Tree measurements were conducted to estimate tree height and volume of each stand (Sect. 2.3.), as these metrics were used in the direct estimation approach of albedo (Sect. 2.5.) and in the statistical analysis (Sect. 2.7.). Within each forest selected, we established one-hectare

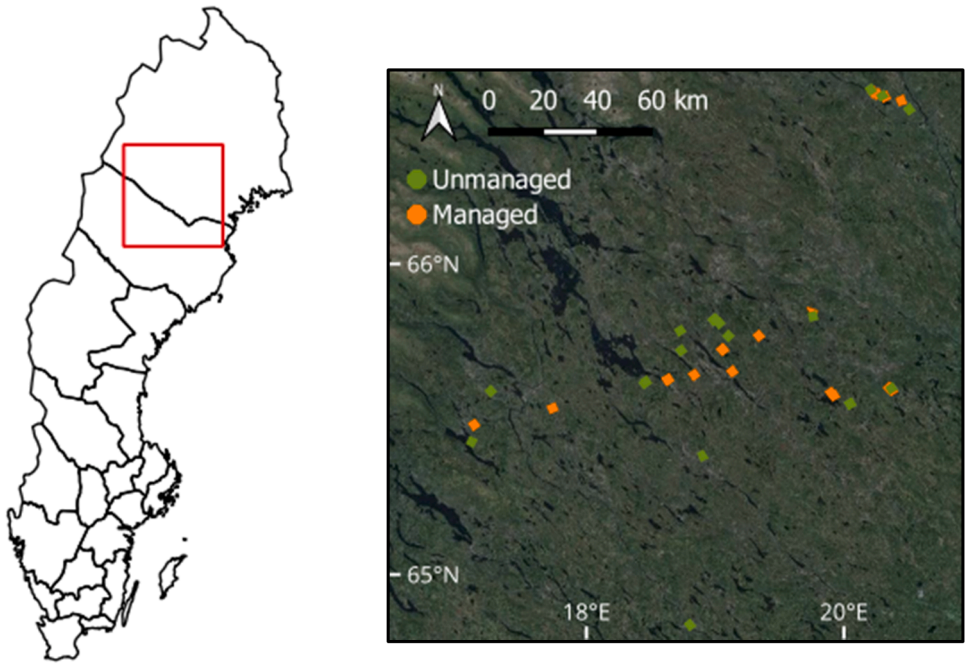

Fig. 1. Location of the study area (red square) in northern Sweden (left), and the distribution of the managed (orange squares) and unmanaged (green squares) forest stands (right).

measurement plots. Within each one-hectare plot, we established five sub-plots with radii of 10 m, one in the center and one in each cardinal direction centered 43.2 m from the forest stand center. For each sub-plot, the diameter at breast height (DBH) of all trees >5 cm was measured for each tree species present. In addition to DBH measurements of all trees, we measured both DBH and height on a sub-set of trees in each plot, so that volume could be estimated from the DBH measurements. Specifically, four sample trees for each of *Pinus, Picea*, and *Betula* were measured for DBH and height using a Nikon Forestry Pro II laser height meter. The sample trees were restricted to trees with a DBH larger than 5 cm, and closest to the plot center. This sampling resulted in a random size distribution for each of the three species in each stand. *Pinus* was the dominant tree species in the study area, and some sub-plots had no sample trees of *Picea* and *Betula*. For a few sub-plots, deciduous species other than *Betula*, such as *Salix, Alnus*, and *Populus*, were present and measured.

2.3. Estimation of Lorey's height and forest volume

Species-specific mean height for *Pinus, Picea*, and *Betula* were estimated as basal area-weighted height, known as Lorey's mean height (Lorey, 1878), for each forest stand. For trees without height measurements, we estimated heights from species-specific diameter-height relationships (Mehtatalo et al., 2015). Due to the low proportion of *Picea* and *Betula* in the focal stands, these relationships were estimated for *Picea* and *Betula* across all forest stands, whereas for *Pinus*, the relationships were estimated individually for each stand. For the youngest unmanaged stand, no living trees were present. Accordingly, to estimate the heights of the remaining dead *Pinus* trees, we used a diameter-height relationship based on sample trees from two other forest stands that deviated less than one year since time of wildfire instead. We considered this reasonable, as the DBH distribution corresponded well between the youngest unmanaged stand and the two forest stands for which the diameter-height relationship was fitted.

Volume per hectare was estimated for *Pinus, Picea*, and *Betula* trees with species-specific volume equations (Brandel, 1990) based on height and DBH as predictor variables. Here, we treated the deciduous tree species other than *Betula* as samples of *Betula*. The height of trees without height measurements was calculated from the diameter-height relationships, as described above. For the three youngest managed stands (less than two years since harvesting), no sample trees were present, and all trees were lower than 1.3 m. Accordingly, we set both volume and Lorey's height to zero for these forest stands.

2.4. Albedo definitions

In the following text, the terms "albedo" and "surface albedo" refer to the ratio reflected to incident solar radiation in the total shortwave region (~0.3–5 μm). In Sect 2.5., we describe how we estimate black-sky and white-sky albedo. Black-sky albedo is the directional-hemispherical reflectance which represents albedo under completely direct illumination conditions (i.e., sun as a point source of illumination), for which the diffuse radiation from the sky is ignored. White-sky albedo is the bihemispherical reflectance which represents albedo under completely isotropic (i.e., directionally independent) illumination. In Sect. 2.6., we described how we calculate the true surface albedo under ambient illumination conditions of both direct and diffuse light, i.e., blue-sky albedo, based on the estimated black-sky and white-sky albedo.

2.5. Direct estimation approach of black- and white-sky albedo

We employed the direct estimation approach based on high-resolution Sentinel-2 satellite imagery described in Bright and Ramtvedt (2024) to estimate black- and white-sky albedo. The 10 m spatial resolution of Sentinel-2 satellite imagery captures reflectance variations according to canopy discontinuities and structural heterogeneity typically present in boreal forests, which overcomes the limitation from previous methods based on coarse-scale satellite products (Cescatti et al., 2012). High-resolution harmonized Sentinel-2 surface reflectance imagery (L2A) were processed and downloaded using the rgee package (Aybar et al., 2020) in R software (R Core Team, 2024). This package calls the Google Earth Engine (GEE) (Gorelick et al., 2017) application programming interface, which allows the performance of GEE analyses using R syntax. Prior to downloading, cloud masking was performed to ensure that only high-quality surface reflectance was used in the estimation. We used a cloud detection algorithm based on the Sentinel-2

cloud probability dataset (s2cloudless) by assuming that pixels classified with cloud probability larger than 40 % were disturbed by low-to-mid atmospheric clouds. Because s2cloudless has no cloud shadow detection and the algorithm is prone to errors on very bright surfaces (Skakun et al., 2022), we further applied the Sentinel-2 cloud displacement index using the Sentinel-2 Level 1C dataset to reduce the chance of false classification of snow surfaces as low clouds (Frantz et al., 2018). Moreover, the shadow of all clouds detected based on the above-mentioned criteria was projected for a diameter of 5000 m. If no Sentinel imagery were available when following the cloud filtering described above, we applied a less aggressive cloud masking by the Sentinel-2 QA60 band (European Space Agency, 2024a) for those pixels determined with <60 % cloud probability according to s2cloudless. Even though the QA60 band has a lower accuracy for cloud detection (Wright et al., 2024), the full cloud filtering procedure reduced the erroneous rejection of clear pixels and the acceptance of cloudy scenes. We downloaded data for a five-year period (2019–2023). For stands where forest fires or clear cuts occurred after 2019, data were downloaded only for the period after the disturbance.

The basis of the direct estimation approach is an angular-bin-based regression connecting Sentinel-2 nadir surface reflectance with intrinsic black- and white-sky albedo for Fennoscandian forests. The angular regression yields a forest class- and solar viewing geometry-dependent look-up table (LUT) database (i.e., reflectance–albedo relationship) for the 10-m resolution near-infrared (NIR) and visible (blue, green, and red) bands. The LUT is divided into forest classes of evergreen needleleaf forests and deciduous broadleaf forests. Accordingly, prior to estimation of surface albedo, each forest stand was classified based on their dominant species-specific volumes. The black- and white-sky albedo were calculated as follows:

$$\alpha_{xSA}(\theta_s, \theta_v, \varphi) = k_0(\theta_s, \theta_v, \varphi) + \sum_{i=1}^{4} k_i(\theta_s, \theta_v, \varphi) \times \rho_{S-2}(\lambda_i) \quad (1)$$

where α_{xSA} is either black- or white-sky albedo, $\rho_{S-2}(\lambda_i)$ is the Sentinel-2-like surface reflectance at spectral band λ_i ($i = 1, 2, 3, 4$), which corresponds to channels 2 (blue; 490 nm), 3 (green; 560 nm), 4 (red; 665 nm), and 8 (NIR; 842 nm). k_0 is a constant fit parameter and k_i is spectral band-specific fit parameters for spectral band λ_i ($i = 1, 2, 3, 4$) (see Bright and Ramtvedt, 2024). θ_s, θ_v, and φ represent the solar zenith, viewing zenith, and relative azimuth angles, respectively. The latter three parameters were obtained from the Sentinel-2 Level 1C metadata. According to terrain slope and azimuth as primary factors affecting albedo in rugged terrain (Ramtvedt and Næsset, 2023), we used the local solar viewing geometry (i.e., relative geometry between terrain slope and solar or viewing sensor) as inputs to identify the LUT angular bin (i.e., θ_s, θ_v, and φ) for each 10-m grid cell within the Sentinel-2 imagery. The terrain slope was calculated based on the 30 m resolution global digital elevation model of Copernicus (European Space Agency, 2024b). We applied resampling based on bilinear interpolation to find terrain slope according to the 10-m grid scale of the Sentinel-2 imagery. Monthly median black- and white-sky albedo were calculated for each stand, by omitting any imagery missing high-quality reflectance according to the cloud filtering procedure.

2.6. Computation of surface albedo

We estimated monthly surface albedo (α) as follows:

$$\alpha = \alpha_{WSA} \times f_{diff} + \alpha_{BSA}\left(1 - f_{diff}\right) \quad (2)$$

where α_{WSA} and α_{BSA} represent the white- and black-sky albedo, respectively, as estimated using Eq. (1). f_{diff} is the fraction of diffuse radiation from the total incoming solar radiation. This was predicted from the clearness index (defined as the ratio of global solar radiation to extraterrestrial radiation) according to the empirical model (Eq. 12) of Ibrahim (1985). This model was chosen because of its simplicity and good performance in climate similar to that of the current study (Despotovic et al., 2016). We calculated average daily extraterrestrial radiation for the middle day of each month, by assuming that this choice of day had the best correspondence with the time of the monthly mean values of the albedo. Average daily global solar radiation was collected from the ERA-5 reanalysis product (Hersbach et al., 2020) of the European Center for Medium-Range Weather Forecasts (ECMWF). The product, which has an improved performance for solar radiation compared to previous versions (Tahir et al., 2021), assimilates model data with observations from across the world with a horizontal resolution of 0.25° × 0.25° We downloaded the mean surface downward shortwave radiation flux averaged monthly for each forest stand location. An assessment of this product has revealed a root mean square error of 10.2 Wm^{-2} for high latitudes (59–70°) (Babar et al., 2019), which was considered satisfactory for use in the current study.

2.7. Statistical analysis

A linear mixed-effects model (LMM) was applied to assess the statistical significance of forest type (i.e., unmanaged versus managed forest) and stand age on albedo. The natural logarithm of annual albedo for the period 2019–2023 was used as a response variable to capture its nonlinear response to forest age (Kuusinen et al., 2014). Moreover, the log-transformation ensured fulfilling the LMM's assumption of constant variance by removing patterns of heteroscedasticity (i.e., non-constant variance of errors). Forest type, stand age, and their interaction were included in the LMM as fixed effects, whereas the five-year period with repeated albedo estimates for each year was included as a random effect. This was done to allow for examination of any potential variation according to year-to-year differences (e.g., such as snow conditions) yet accounting for the within-stand dependency among the albedo estimates. Modelling assumptions were checked to ensure validity and reliability of their results. The LMM was fitted with the restricted maximum likelihood (Patterson and Thompson, 1971) using the lme4 package (Bates et al., 2015) in the R software (R Core Team, 2024). We used the Satterthwaite approximation (Satterthwaite, 1941) to evaluate the significance of the fixed effects. This approximation has been found to be most suitable with Type 1 error rates close to 0.05 when using the restricted maximum likelihood, even for smaller samples (Luke, 2017). We reported the dependency between albedo and the fixed effects in terms of the marginal (R_m^2) and conditional (R_c^2) determination coefficients (Nakagawa and Schielzeth, 2013). R_m^2 can be interpreted as the proportion of albedo variability explained by the given fixed effects in the model, whereas R_c^2 gives the total variance explained by the model. The relative contribution of each fixed effect on albedo variability was determined according to Lai et al. (2022). According to violations of normality and homoscedasticity, we applied a permutation test (Wheeler et al., 2022) based on analysis of variance to determine whether the albedo of managed and unmanaged forests differed significantly from each other. Furthermore, correlation analysis of albedo, stand age, and volume was conducted to understand the potential differences between the effects of forest disturbances and the development of stand age and volume on albedo.

3. Results

3.1. Albedo dynamics during stand development

Overall, the mean annual albedo over the whole chronosequence was significantly lower ($p < 0.05$) for unmanaged forests (0.17±0.05) than managed forests (0.23±0.10). Such a direct comparison should be conducted carefully because managed forests span 1–109 years, whereas unmanaged forests span 4–375 years. However, because both chronosequences are represented with the same number of observations,

being evenly spaced within their respective age spans, a direct comparison was considered valid. Visual inspection of the albedo data showed that managed forests had a consistently decreasing albedo trend throughout the entire stand development (Fig. 2), whereas this pattern was not apparent in the unmanaged forests (Fig. 2). By dividing the two chronosequences into young (<30 years) and mature forests (>30 years), we reveal that the annual albedo for young managed forests (0.36±0.04) is twice as large as that of young unmanaged forests (0.18 ±0.04), whereas in mature forests, the albedo of managed stands (0.17 ±0.03) is only slightly larger (approximately 6 %) than that of unmanaged stands (0.16±0.05).

Based on the LMM, we find that forest type (i.e., managed or unmanaged forests), stand age since disturbance, and their interactions all significantly affect albedo (Table 1). Overall, the predictors explain 90 % of the variation in albedo, for which the fixed effects constitute 58 %. Forest type and the interaction between stand age and forest type are the two most important factors explaining changes in albedo after disturbance, with relative contributions of 31 % and 51 %, respectively, of the total variance explained by the fixed effects (Table 1). We further observe that 77 % of the remaining variance (i.e., the variance not explained by forest type and stand age) was explained by interannual differences in albedo, which is mainly a function of variation in snow cover.

We find the largest decrease in managed boreal albedo as young stands transition to mature closed canopy stands, approximately 30 years after clear-cutting (Fig. 2). Based on LMM estimates, albedo in unmanaged forests surpasses that in managed forests ~72 years after initial disturbance (Fig. 2). Even though LMM estimates reveal a decline in albedo following time since disturbance in unmanaged forests, the actual observations show a slight increase in albedo from around 200 years after fire (0.12±0.02) towards the oldest stand of 375 years (0.17 ±0.02) (Fig. 2).

3.2. Seasonal differences in albedo

Given that snow has a considerably higher albedo than coniferous trees, we divided the full dataset into subgroups of summer and winter observations to distinguish between seasonal differences. Observations from October to May were considered winter albedo because visual inspection revealed that in most of these months, snow was present in the stands. Summer albedo was considered as observations from June to September. The large positive Δalbedo at younger ages (Fig. 2), were mainly caused by higher winter albedo in clear-cut stands compared to that in post-fire stands (Fig. 3).

Focusing on seasonal dynamics, it becomes evident that the largest seasonal shift in albedo occurs during snow-melting from April to May, whereas the largest among-stand albedo difference is found in the period from February to April (Fig. 3). As expected, the magnitude of albedo declines during snowmelt decreased over time after disturbance, meaning that albedo of mature high-density forest stands is less sensitive to snowmelt during spring than young stands with a lower fraction of canopy cover. By comparing the seasonal albedo dynamics for managed stands (Fig. 3a) versus unmanaged stands (Fig. 3b), we observe that the pattern of declining albedo with increasing time since disturbance in managed forests is not present for winter months in unmanaged forests. Specifically, our data shows a weaker relationship between time since disturbance and stand volume for unmanaged forests than for managed forests, with relatively stable stand volumes for unmanaged stands approximately 100 years of age and older (Fig. 4a). The less pronounced pattern between stand development and volume for unmanaged forests weakens the dependency between albedo and time since disturbance for that forest type (Fig. 4b).

During summer, we find the lowest albedo in unmanaged forests (0.07±0.006) in the first year after the fire event. While summer albedo in unmanaged forests remains unchanged during stand development (Fig. 3b), summer albedo in managed forests shows a decreasing trend as the stands become older (Fig. 4a). Even-aged management results in clear-cuts that are dominated by birch trees and understory plants, which influences the summer albedo in most years immediately after clear-cutting (<10 years), but also during the gradual transition from deciduous to *Pinus* trees in the young forest.

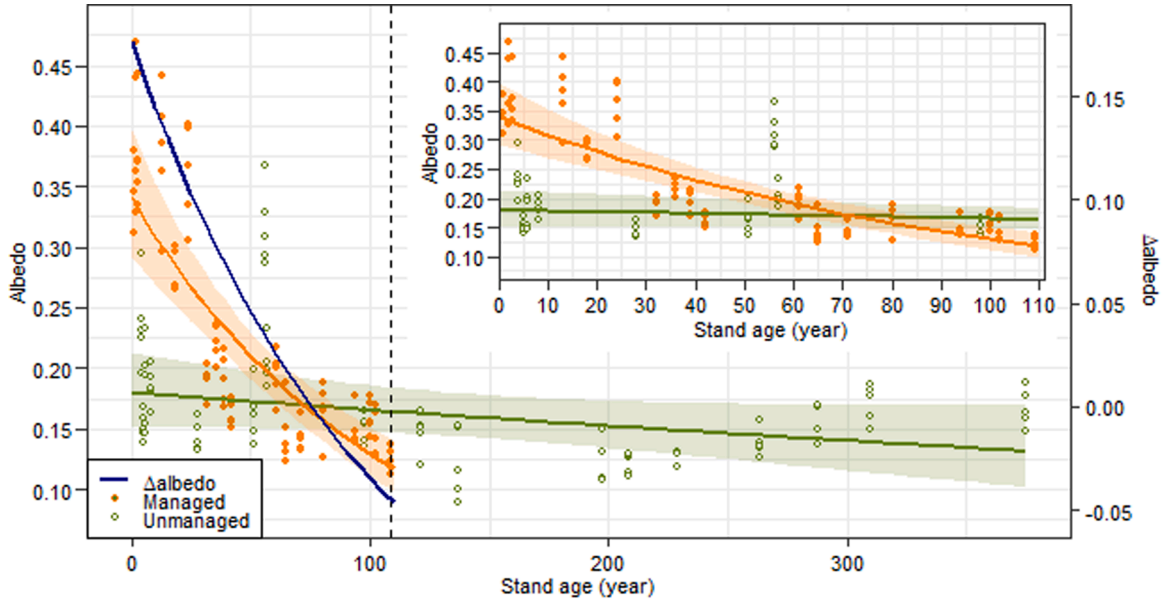

Fig. 2. Comparison of albedo for chronosequences of managed (orange dots) and unmanaged (green circles) forests for different stand ages on a mean annual basis for the period 2019–2023. The lines represent the estimated fit according to the LMM, with shaded regions representing the 95 % confidence interval. Δalbedo represents the difference between estimated albedo of managed and unmanaged forests. The dashed vertical line indicates the age of the oldest managed stand included in the study. The inserted figure represents the comparison of albedo for only the first 110 years (i.e., corresponding to the observations to the left of the dashed vertical line).

Table 1
Summary of LMM fitted for the natural logarithm of albedo as response variable and forest type (i.e., managed versus unmanaged forests) and age as fixed effects. SE denotes the standard error of the predictor estimates. Relative R_m^2 represents the relative contribution of each predictor to the total variance explained by all fixed effects (R_m^2).
R_c^2 denotes the conditional determination coefficient, indicating the total variance in albedo explained by the LMM. Random effect represents the percentage variance explained by year-to-year differences in the remaining variance that is not accounted for by the fixed effects.

Predictor	SE	t-value	p	Relative R_m^2 (%)	R_m^2	R_c^2	Random effect (%)
Forest type	0.117	−5.444	5.3×10^{-6}	31.3			
Age	0.001	−6.760	1.2×10^{-7}	17.7	0.58	0.90	76.7
Interaction	0.001	5.907	1.4×10^{-6}	51.0			

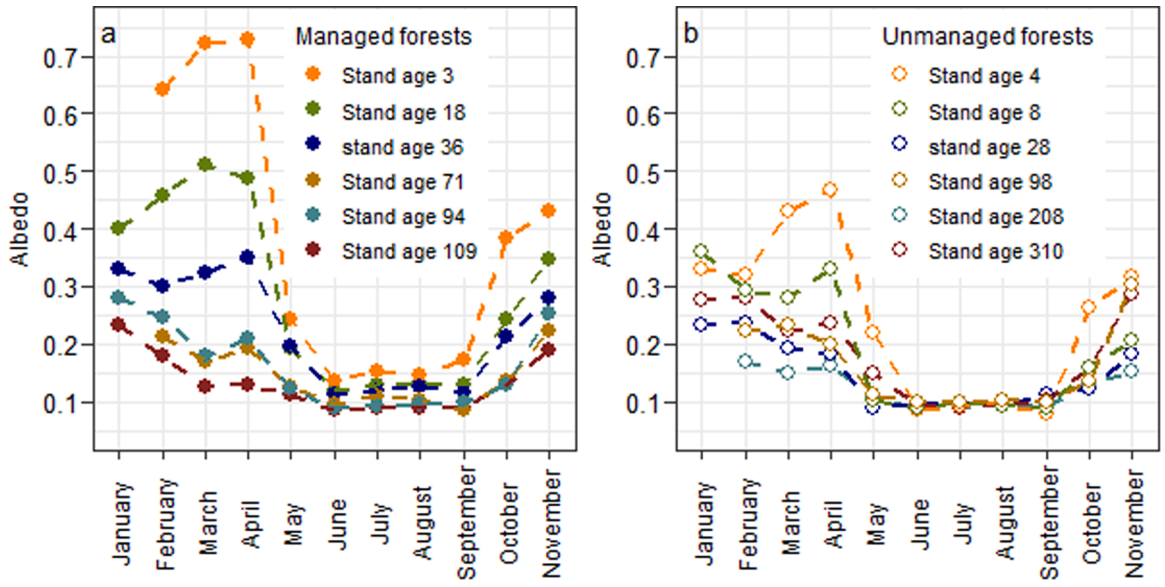

Fig. 3. Monthly mean albedo based on all five years (2019–2023) for selected stand ages of managed forests (a) and unmanaged forests (b). It should be noted that albedo observations for some stands in January are missing due to lack of high-quality satellite observations during this month (see Sect. 2.5.).

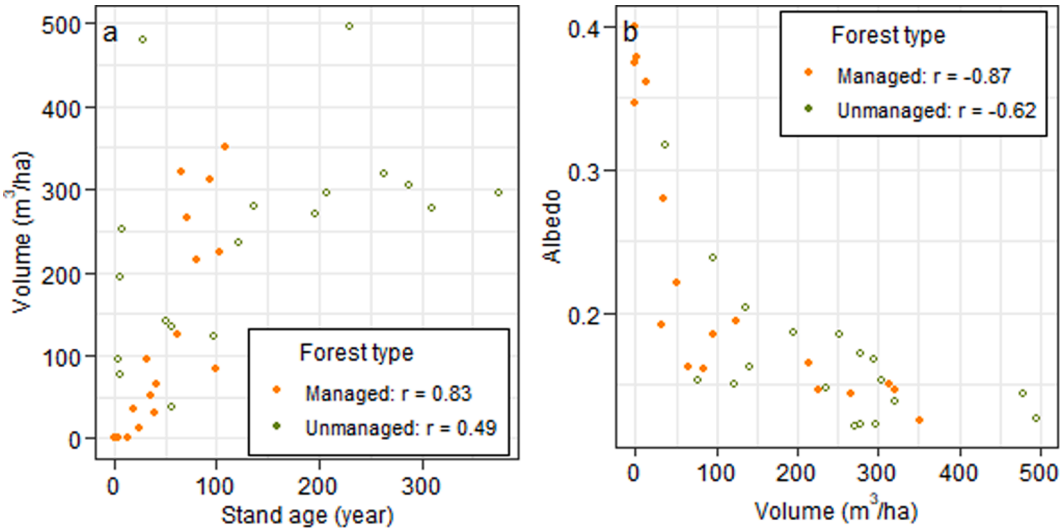

Fig. 4. Relationships between stand age and volume (a), and volume and albedo (b). r represents Pearson correlation coefficient.

4. Discussion

4.1. Impact of snow cover on albedo

Our results revealed that the largest seasonal shift in albedo occurred during snow-melting from April to May, whereas the largest among-stand albedo difference was found in the period from February to April (Fig. 3). This coincided well with the results reported for 11 managed sites in Finland and Sweden, with latitudes ranging from 63 to 69° (Hovi et al., 2019).

As shown in Fig. 3b, we found no consistent trend in albedo with increasing age in unmanaged forests during winter. This can be related

to previous research which has revealed that the presence of snow has a small effect on albedo when forest canopies cover >70 % of the ground (Ni and Woodcock, 2000), and that the albedo of coniferous forests shows substantial variation due to differences in canopy shading (Webster and Jonas, 2018). Because unmanaged forests show larger structural heterogeneity (Langridge et al., 2023) with larger variability in canopy discontinuities and tree size arrangements, the effect of canopy shading complicates the radiation regime within these forest stands.

The overall goal of the current study was to examine how albedo develops over time after wildfires and clear-cutting. Accordingly, the impact of snow cover on albedo, such as the temporal distribution of snow in the canopy, was not examined separately but treated as a part of the overall forest reflectance. Annual differences in snow cover were present in the different stands included in the study (indicated by the observations in Fig. 2 and the random effect in Table 1). However, given that the mean estimates were based on five years of satellite data, random year-to-year differences are unlikely to explain systematic albedo differences between stands. Moreover, potential spatial differences in snow cover were considered negligible, given the relatively small study region with similar climatic conditions. We recommend further research to examine how dynamics and differences in snow cover impact winter albedo in managed and unmanaged boreal forests, particularly under global warming with an expected reduced albedo during spring due to earlier snow-melting.

4.2. Impact of forest fire severity on albedo

We found the lowest summer albedo in unmanaged forests in the first year after the fire event, highlighting the strong reduction in albedo due to charcoal residues after wildfire in unmanaged forests (Amiro et al., 2006; Lyons et al., 2008). Even though there is substantial variability in the severity of wildfires among the unmanaged forest stands included in the current study, we observed that only a partial reduction in volume occurred in response to fire (Fig. 4a). Most of these reductions are related to perturbations in canopy cover, with large parts of the standing stem volume remaining after the fire events (Fig. 4a.). Despite the strong sensitivity of winter albedo to canopy cover (Webster and Jonas, 2018), our results revealed that the remaining charred standing tree stems (snags) from the high-severity fire in the youngest unmanaged stand (Fig. 4a) considerably decreased the winter albedo compared to that of clear-cutting (Fig. 3). Snags have been found to potentially be the dominant controller of post-fire albedo on decadal timescales (O'Halloran et al., 2014). Particularly during winter when snow is present, the role of snags on albedo is dependent on fire severity, snag-fall rate, and the time required for seedlings and saplings to grow tall enough to protrude above the snow cover (O'Halloran et al., 2014). Further research is needed to fully understand the role of snags on albedo with altered fire regimes and snow conditions under projected climate changes. As pointed out by Halim et al. (2019), the presence of both black carbon (charcoal and soot) and charred branches and stems protruding through snow can contribute to lowering albedo immediately after stand-replacing fires and during late spring and/or early winter. We found that the post-fire winter albedo of young stands reported here is generally lower than that reported for wildfire-disturbed stands located at northern latitudes of 53–63° in Canada and Alaska, where high-severity fires are more common (Amiro et al., 2006). These albedo differences are likely caused by the interplay between fire severity and differences in dominant tree species in North America compared to Europe. *Pinus*-dominated forests, as studied here, are relatively fire-resistant and less prone to crown fires than the *Picea*-dominated forests in North America. Less intensive wildfires, with less destroyed living vegetation and fewer killed trees, can result in substantially lower albedo compared to high-severity fires within unmanaged forests (Rogers et al., 2015). However, the cooling albedo effect from high-severity wildfires is likely to decrease in future decades owing to the reduced snow cover in spring months with climate change (Potter et al., 2019).

4.3. Implications on albedo if converting rotational management to unmanaged forests

Whereas past forest management practices were primarily driven by economic factors and considerations related to woody biomass, today's management practices must increasingly address additional forest values, such as biodiversity, climate benefits, and recreation (Mason et al., 2022). In Europe, the new EU forest strategy for 2030 aims to improve the quantity and quality of forests (European Commission, 2021). Measures promoting the protection of the EU's remaining primary old-growth forests and sustainable forest management, e.g., avoiding clear-cutting, among others, are proposed in the strategy. A relevant question in this context is how the surface albedo of northern boreal forests can be affected by such strategies. Accordingly, we performed a scenario in which managed forest stands subjected to clear-cutting with rotation length varying from 50 to 110 years were replaced by unmanaged forests with wildfire frequency in the range of 60–375 years. This was based on predictions using LMM estimates for every fifth year. The rotation lengths were chosen based on typical rotation lengths in boreal Fennoscandia (Roberge et al., 2016; Stokland, 2021).

These scenarios showed that converting managed forests into an old unmanaged state generally will reduce albedo (Fig. 5a). Scenarios in which clear-cut managed forests with short rotation lengths (50–70 years) are replaced by unmanaged forests with low wildfire frequency (250–375 years), will result in a substantial cumulative albedo decrease (>81 % (Fig. 5b)). Furthermore, we observed that albedo will increase modestly (<0.06) only in the scenario where unmanaged forests with wildfire frequency ≤60 years replaced managed forests aged >81 years (Fig. 5a). Our scenario provides important novel insights into potential albedo changes, with mainly associated negative climate impacts, if clear-cut managed stands are replaced by unmanaged forests. However, it is important to emphasize that future boreal forest management requires a careful assessment of the multidimensional roles of forests, such as carbon sequestration, timber production, and biodiversity. Simulation studies in Finland have shown that unmanaged *Picea* stands result in a net climatic cooling effect compared to forest management, with the effect of increased carbon stocks surpassing that of changes in surface albedo (Kellomäki et al., 2021; 2023). However, this carbon–albedo tradeoff was not compensated for loss of no harvest and the potentially avoided emissions due to wood material and energy substitution. We note that the scenarios presented here were based on a small dataset, and the forest types included are not necessarily universal for other types of boreal forests. Further, the scenarios were based on current forest states, and no adaptations were made to correct for potential future changes. The implications of management regimes on albedo under forest conversion are likely to change under future global warming, due to the increased probability of fires (Kinnunen et al., 2024) and shorter periods of snow cover (Mellander et al., 2007) in the current century in Fennoscandia. For example, if snow cover declines due to climate warming, then young managed stands will likely have a weaker cooling effect, reducing the albedo difference between managed and unmanaged forests. Moreover, with rising temperatures, which are increasing faster in the boreal biome than in any other forested region (Gauthier et al., 2015), rotation lengths of high-latitude boreal-managed forests may become shorter in the future to maintain productivity (Kellomäki et al., 2008). This could increase the cooling effect of managed forests relative to unmanaged forests.

4.4. Discussion of albedo effect in continuous cover forestry

As an alternative to clear-cut rotational management, harvesting methods such as continuous cover forestry (Pommering and Murphy, 2004) have attracted increasing interest in many European countries to

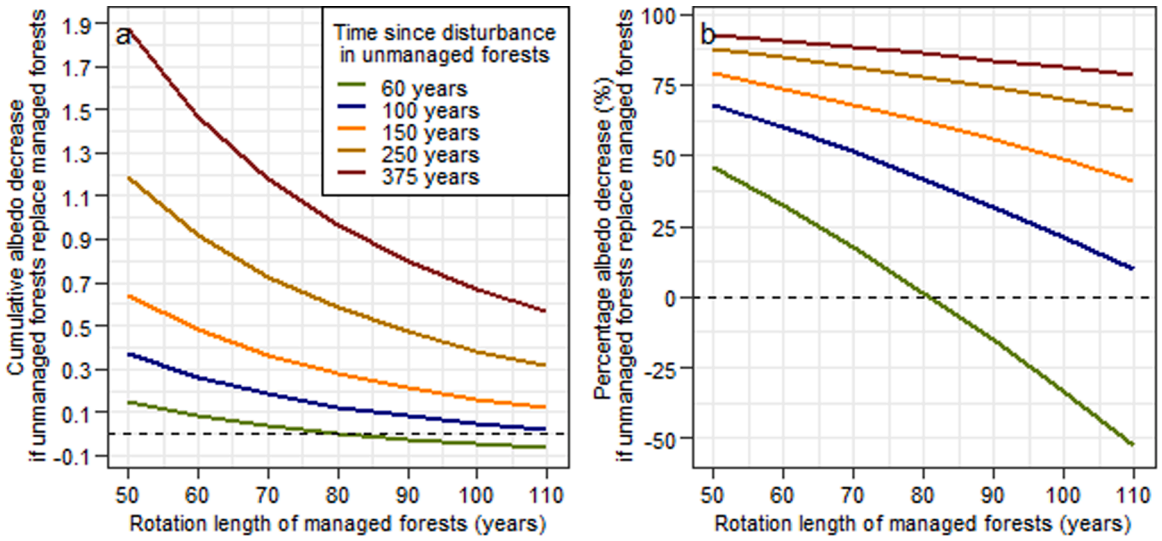

Fig. 5. Scenarios of mean cumulative albedo decrease (a) and the corresponding percentage decrease (b) if replacing clear-cut managed forests by unmanaged boreal forests. The scenarios are based on predictions from the LMM. Negative values represent an increase in albedo.

meet the demand for a wider range of ecosystem services (Mason et al., 2022). The concept of continuous and uninterrupted forest maintenance aligns with closer-to-nature management by promoting structural diversity, canopy heterogeneity, and natural regeneration cycles, similar to those found in old-growth unmanaged forests. Apart from two studies that simulated albedo for even-aged versus uneven-aged *Picea* stands (Kellomäki, et al., 2021; 2023), no studies have reported the albedo effect in boreal forest stands managed with continuous cover forestry. Applying the key findings of the observation-driven analysis we performed here, suggests that replacing clear-cutting practices with continuous cover forestry would likely decrease surface albedo substantially. According to our results, this is mainly due to the omission of prolonged winter periods of high albedo, such as those observed in young, clear-cut forests during stand re-establishment. It is well established that albedo generally decreases as volume (Fig. 4), tree height, and canopy cover increase (Hovi et al., 2019; Kuusinen et al., 2016; Lukeš et al., 2013). Therefore, explicit consideration of albedo is warranted alongside more commonly measured greenhouse gases when determining the overall climate benefits of different forest management practices. Greater inclusion of deciduous species in commercial forestry across Fennoscandia could offer one method to maximize wood production and carbon uptake whilst simultaneously increasing albedo during winter (Dubois et al., 2020). Moreover, studies have shown that the vertical distribution of biological matter significantly influences albedo (Ramtvedt et al., 2024), with highly hierarchical clumped structures increasing the chances of photons being trapped within shoots and crowns (Rautiainen and Stenberg, 2005). Despite this, limited research has been conducted on how within-stand structural heterogeneity and the three-dimensional spatial arrangement of canopy characteristics impact the overall stand albedo. Acquiring this knowledge is essential for a better understanding of the albedo of structurally heterogeneous old-growth unmanaged forests and the potential effects of adopting continuous cover forestry as the standard for boreal forest management.

5. Conclusion

This study used a space-for-time approach to compare temporal changes in albedo during stand development between unmanaged and managed boreal forests, based on high-resolution observational data from Sentinel-2 reflectance imagery. We established two chronosequences in *Pinus*-dominated forests in northern Sweden: one in unmanaged wildfire-disturbed forests spanning 4–375 years and the other in managed clear-cut rotation forests spanning 1–109 years. Our results show that albedo decreases over time after disturbance, but mainly in managed forests. This decrease was mainly driven by the markedly lower albedo in young (<30 years) unmanaged post-fire forests (0.18±0.04) compared to that of young clear-cut managed forests (0.36±0.04). The mean albedo over the entire unmanaged chronosequence (0.17±0.05) was significantly lower ($p < 0.05$) than that of the managed chronosequence (0.23±0.10). To find optimal solutions that maximize the ecosystem services provided by boreal forests, such as biomass production, biodiversity, and climate benefits, our results emphasize the need to incorporate albedo considerations into the overall assessment, to better understand the relationships and tradeoffs among these multiple forest attributes.

Data availability

Sentinel-2 data, digital terrain data, and average daily global solar radiation are available at https://dataspace.copernicus.eu/. Field data are available from the corresponding author or Michael J. Gundale on reasonable request.

CRediT authorship contribution statement

Eirik Næsset Ramtvedt: Writing – review & editing, Writing – original draft, Visualization, Methodology, Investigation, Formal analysis, Data curation. **Ryan M. Bright:** Writing – review & editing, Methodology. **Terje Gobakken:** Writing – review & editing, Project administration, Data curation. **Adrián Cidre-González:** Writing – review & editing, Data curation. **Maja K. Sundqvist:** Writing – review & editing, Conceptualization. **Zsofia R. Stangl:** Writing – review & editing, Conceptualization. **Marie-Charlotte Nilsson:** Writing – review & editing, Conceptualization. **Daniel B. Metcalfe:** Writing – review & editing, Conceptualization. **Michael J. Gundale:** Writing – review & editing, Project administration, Funding acquisition, Conceptualization.

Declaration of competing interest

The authors declare that they have no know competing financial interests or personal relationships that could have appeared to influence the work reported in this paper.

Acknowledgements

This study was supported by a grant from Swedish Formas (Formas

D-nr 2021-02116), awarded to M.J.G, and by the Norwegian University of Life Sciences. R.M.B. received additional support from the Research Council of Norway (grant number 302701).

Supplementary materials

Supplementary material associated with this article can be found, in the online version, at doi:10.1016/j.agrformet.2025.110924.

References

Ahlström, A., Canadell, J.G., Metcalfe, D.B., 2022. Widespread unquantified conversion of old boreal forests to plantations. Earth's Future 10 (11). https://doi.org/10.1029/2022EF003221 e2022EF003221.

Amiro, B., Orchansky, A.L., Barr, A.G., Black, T.A., Chambers, S.D., Chapin Iii, F.S., Goulden, M.L., Litvak, M., Liu, H.P., McCaughey, J.H., McMillian, A., Randerson, J. T., 2006. The effect of post-fire stand age on the boreal forest energy balance. Agric. For. Meteorol. 140 (1–4), 41–50. https://doi.org/10.1016/j.agrformet.2006.02.014.

Aybar, C., Wu, Q., Bautista, L., Yali, R., Barja, A., 2020. rgee: an R package for interacting with Google Earth Engine. J. Open Source Softw. 5 (51), 2272.

Babar, B., Graversen, R., Boström, T., 2019. Solar radiation estimation at high latitudes: assessment of the CMSAF databases, ASR and ERA5. Sol. Energy 182, 397–411. https://doi.org/10.1016/j.solener.2019.02.058.

Bates, D., Machler, M., Bolker, B., Walker, S., 2015. Fitting linear mixed-effects models using lme4. J. Stat. Softw. 67 (1). https://doi.org/10.18637/jss.v067.i01.

Bonan, G.B., 2008. Forests and climate change: forcings, feedbacks, and the climate benefits of forests. Science 320 (5882), 1444–1449. https://doi.org/10.1126/science.1155121.

Bradshaw, C.J., Warkentin, I.G., 2015. Global estimates of boreal forest carbon stocks and flux. Glob. Planet. Change 128, 24–30. https://doi.org/10.1016/j.gloplacha.2015.02.004.

Bradshaw, C.J., Warkentin, I.G., Sodhi, N.S., 2009. Urgent preservation of boreal carbon stocks and biodiversity. Trends Ecol. Evol. 24 (10), 541–548. https://doi.org/10.1016/j.tree.2009.03.019.

Brandel G.: Volymfunktioner för enskilda träd. Tall, gran och björk. [Volume functions for individual trees: scots pine (Pinus sylvestris), Norway spruce (Picea abies) and birch (Betula pendula & Betula pubescens)]. Sveriges Lantbruksuniversitet, Inst f skogsproduktion, Rapport nr 26, Garpenberg. 1990.

Brassard, B.W., Chen, H.Y., 2008. Effects of forest type and disturbance on diversity of coarse woody debris in boreal forest. Ecosystem 11, 1078–1090. https://doi.org/10.1007/s10021-008-9180-x.

Brassard, B.W., and Chen, H.: Stand structure and composition dynamics of boreal mixedwood forest: implications for forest management. 2010.

Bright, R.M., Astrup, R., 2019. Combining MODIS and national land resource products to model land cover-dependent surface albedo for Norway. Remote Sens. 11 (7). https://doi.org/10.3390/rs11070871.

Bright, R.M., Lund, M.T., 2021. CO_2-equivalence metrics for surface albedo change based on the radiative forcing concept: a critical review. ACP 21 (12), 9887–9907. https://doi.org/10.5194/acp-21-9887-2021.

Bright, R.M., Ramtvedt, E.N., 2024. Compositional and structural stratification does not improve direct estimation of Sentinel-2-derived surface albedo in Fennoscandian forests. Agric. For. Meteorol. 358, 110251. https://doi.org/10.1016/j.agrformet.2024.110251.

Bright, R.M., Astrup, R., Strømman, A.H., 2013. Empirical models of monthly and annual albedo in managed boreal forests of interior Norway. Clim. Change 120 (1–2), 183–196. https://doi.org/10.1007/s10584-013-0789-1.

Bright, R.M., Anton-Fernandez, C., Astrup, R., Cherubini, F., Kvalevag, M., Stromman, A. H., 2014. Climate change implications of shifting forest management strategy in a boreal forest ecosystem of Norway. Glob. Chang. Biol. 20 (2), 607–621. https://doi.org/10.1111/gcb.12451.

Bright, R.M., Cattaneo, N., Antón-Fernández, C., Eisner, S., Astrup, R., 2024. Relevance of surface albedo to forestry policy in high latitude and altitude regions may be overvalued. Environ. Res. Lett. 19 (9), 094023. https://doi.org/10.1088/1748-9326/ad657e.

Buness, V., Sundqvist, M.K., Ali, S.T., Annighöfer, P., Aragon, C.M., Lanzrein, I., Metcalf, D.B., Nilsson, M.-C., Gundale, M.J., 2025. Resource quantity and heterogeneity drive successional plant diversity in managed and unmanaged boreal forests. Ecography, e07676. https://doi.org/10.1111/ecog.07676.

Cescatti, A., Marcolla, B., Santhana Vannan, S.K., Pan, J.Y., Román, M.O., Yang, X., Ciais, P., Cook, R.B., Law, B.E., Matteucci, G., Migliavacca, M., Moors, E., Richardson, A.D., Seufert, G., Schaaf, C.B., 2012. Intercomparison of MODIS albedo retrievals and in situ measurements across the global FLUXNET network. Remote Sens. Environ. 121, 323–334. https://doi.org/10.1016/j.rse.2012.02.019.

Despotovic, M., Nedic, V., Despotovic, D., Cvetanovic, S., 2016. Evaluation of empirical models for predicting monthly mean horizontal diffuse solar radiation. Renew. Sustain. Energy Rev. 56, 246–260. https://doi.org/10.1016/j.rser.2015.11.058.

Dubois, H., Verkasalo, E., Claessens, H., 2020. Potential of birch (Betula pendula Roth and B. pubescens Ehrh.) for forestry and forest-based industry sector within the changing climatic and socio-economic context of Western Europe. Forests 11 (3), 336. https://doi.org/10.3390/f11030336.

European Commission: New EU Forest Strategy for 2030. Communication form the Commission to the European Parliament, the Counsil, the European Economic and Social Committee and the Committee of the Regions, COM(2021) 572 final; European Commission: Brussels, Belgium, 2021.

European Space Agency, 2024a. Level-1C cloud masks – Sentinel-2 MSI technical Guide – Sentinel Online [WWW Document]. Sentin. Online. URL. https://sentiwiki.copernicus.eu/web/s2-processing#S2Processing-CloudMasks (accessed 29.08.2024).

European Space Agency, 2024b Copernicus Global Digital Elevation Model. Distributed by OpenTopography. https://doi.org/10.5069/G9028PQB (accessed 18.09.2024).

Eyvindson, K., Repo, A., Mönkkönen, M., 2018. Mitigating forest biodiversity and ecosystem service losses in the era of bio-based economy. For. Policy Econ. 92, 119–127. https://doi.org/10.1016/j.forpol.2018.04.009.

FAO 2015 Global Forest Resources Assessment 2015: how have the world's forests changed? FAO.

Flannigan, M., Cantin, A.S., De Groot, W.J., Wotton, M., Newbery, A., Gowman, L.M., 2013. Global wildland fire season severity in the 21st century. For. Ecol. Manag. 294, 54–61. https://doi.org/10.1016/j.foreco.2012.10.022.

Frantz, D., Haß, E., Uhl, A., Stoffels, J., Hill, J., 2018. Improvement of the Fmask algorithm for Sentinel-2 images: separating clouds from bright surfaces based on parallax effects. Remote Sens. Environ. 215, 471–481. https://doi.org/10.1016/j.rse.2018.04.046.

Gauthier, S., Bernier, P., Kuuluvainen, T., Shvidenko, A.Z., Schepaschenko, D.G., 2015. Boreal forest health and global change. Science 349 (6250), 819–822. https://www.science.org/doi/epdf/10.1126/science.aaa9092.

Gorelick, N., Hancher, M., Dixon, M., Ilyushchenko, S., Thau, D., Moore, R., 2017. Google Earth Engine: planetary-scale geospatial analysis for everyone. Remote Sens. Environ. 202, 18–27. https://doi.org/10.1016/j.rse.2017.06.031.

Halim, M.A., Chen, H.Y., Thomas, S.C., 2019. Stand age and species composition effects on surface albedo in a mixedwood boreal forest. Biogeosciences 16 (22), 4357–4375. https://doi.org/10.5194/bg-16-4357-2019.

Hasler, N., Williams, C.A., Denney, V.C., Ellis, P.W., Shrestha, S., Terasaki Hart, D.E., Wolff, N.H., Yeo, S., Crowther, T.W., Werden, L.K., Cook-Patton, S.C., 2024. Accounting for albedo change to identify climate-positive tree cover restoration. Nat. Commun. 15 (1), 2275. https://doi.org/10.1038/s41467-024-46577-1.

Hersbach, H., Bell, B., Berrisford, P., Hirahara, S., Horányi, A., Munoz-Sabater, J., Thépaut, J.-N., 2020. The ERA5 global reanalysis. Q. J. R. Meteorol. Soc. 146 (730), 1999–2049. https://doi.org/10.1002/qj.3803.

Hovi, A., Liang, J., Korhonen, L., Kobayashi, H., Rautiainen, M., 2016. Quantifying the missing link between forest albedo and productivity in the boreal zone. Biogeosciences 13 (21), 6015–6030. https://doi.org/10.5194/bg-13-6015-2016.

Hovi, A., Lindberg, E., Lang, M., Arumäe, T., Peuhkurinen, J., Sirparanta, S., Pyankov, S., Rautiainen, M., 2019. Seasonal dynamics of albedo across European boreal forests: analysis of MODIS albedo and structural metrics from airborne LiDAR. Remote Sens. Environ. 224, 365–381. https://doi.org/10.1016/j.rse.2019.02.001.

Ibrahim, S.M., 1985. Diffuse solar radiation in Cairo, Egypt. Energy Convers. Manag. 25 (1), 69–72. https://doi.org/10.1016/0196-8904(85)90072-X.

Jones, M.W., Kelley, D.I., Burton, C.A., Di Giuseppe, F., Barbosa, M.L.F., Brambleby, E., McNorton, J.R., 2024. State of wildfires 2023–2024. Earth Syst. Sci. Data 16 (8), 3601–3685. https://doi.org/10.5194/essd-16-3601-2024.

Kellomäki, S., Peltola, H., Nuutinen, T., Korhonen, K.T., Strandman, H., 2008. Sensitivity of managed boreal forests in Finland to climate change, with implications for adaptive management. Philos. Trans. R. Soc. B: Biol. Sci. 363 (1501), 2339–2349. https://doi.org/10.1098/rstb.2007.2204.

Kellomäki, S., Väisänen, H., Kirschbaum, M.U., Kirsikka-Aho, S., Peltola, H., 2021. Effects of different management options of Norway spruce on radiative forcing through changes in carbon stocks and albedo. Forestry 94 (4), 588–597. https://doi.org/10.1093/forestry/cpab010.

Kellomäki, S., Strandman, H., Kirsikka-Aho, S., Kirschbaum, M.U., Peltola, H., 2023. Effects of thinning intensity and rotation length on albedo-and carbon stock-based radiative forcing in boreal Norway spruce stands. Forestry 96 (4), 518–529. https://doi.org/10.1093/forestry/cpac058.

Kinnunen, O., Backman, L., Aalto, J., Aalto, T., Markkanen, T., 2024. Projected changes in forest fire season, the number of fires, and burnt area in Fennoscandia by 2100. Biogeo 21 (21), 4739–4763. https://doi.org/10.5194/bg-21-4739-2024.

Kuusinen, N., Tomppo, E., Shuai, Y., Berninger, F., 2014. Effects of forest age on albedo in boreal forests estimated from MODIS and Landsat albedo retrievals. Remote Sens. Environ. 145, 145–153. https://doi.org/10.1016/j.rse.2014.02.005.

Kuusinen, N., Stenberg, P., Korhonen, L., Rautiainen, M., Tomppo, E., 2016. Structural factors driving boreal forest albedo in Finland. Remote Sens. Environ. 175, 43–51. https://doi.org/10.1016/j.rse.2015.12.035.

Lai, J., Zou, Y., Zhang, S., Zhang, X., Mao, L., 2022. glmm. Hp: an R package for computing individual effect of predictors in generalized linear mixed models. J. Plant Ecol. 15 (6), 1302–1307. https://doi.org/10.1093/jpe/rtac096.

Langridge, J., Delabye, S., Gilg, O., Paillet, Y., Reyjol, Y., Sordello, R., Touroult, J., Gosselin, F., 2023. Biodiversity responses to forest management abandonment in boreal and temperate forest ecosystems: a meta-analysis reveals an interactive effect of time since abandonment and climate. Biol. Conserv., 110296 https://doi.org/10.1016/j.biocon.2023.110296.

Lindahl, K.B., Sténs, A., Sandström, C., Johansson, J., Lidskog, R., Ranius, T., Roberge, J.-M., 2017. The Swedish forestry model: more of everything? For. Policy Econ. 77, 44–55. https://doi.org/10.1016/j.forpol.2015.10.012.

Lorey, T.: Die mittlere bestandeshöhe. Allgemeine Forst-und jagdzeitung 54, 149–155. 1878.

Luke, S.G., 2017. Evaluating significance in linear mixed-effects models in R. Behav. Res. Methods 49, 1494–1502. https://doi.org/10.3758/s13428-016-0809-y.

Luyssaert, S., Schulze, E.-D., Börner, A., Knohl, A., Hessenmöller, D., Law, B.E., Ciais, P., Grace, J., 2008. Old-growth forests as global carbon sinks. Nature 455 (7210), 213–215. https://doi.org/10.1038/nature07276.

Lyons, E.A., Jin, Y., Randerson, J.T., 2008. Changes in surface albedo after fire in boreal forest ecosystems of interior Alaska assessed using MODIS satellite observations. J. Geophys. Res. Biogeo. 113 (G2). https://doi.org/10.1029/2007JG000606.

Lukeš, P., Stenberg, P., Rautiainen, M., 2013. Relationship between forest density and albedo in the boreal zone. Ecol. Modell. 261-262, 74–79. https://doi.org/10.1016/j.ecolmodel.2013.04.009.

Mackey, B., DellaSala, D.A., Kormos, C., Lindenmayer, D., Kumpel, N., Zimmerman, B., Hugh, S., Young, V., Foley, S., Arsenis, K., Watson, J.E.M., 2015. Policy options for the world's primary forests in multilateral environmental agreements. Conserv. Lett. 8 (2), 139–147. https://doi.org/10.1111/conl.12120.

Mason, W.L., Diaci, J., Carvalho, J., Valkonen, S., 2022. Continuous cover forestry in Europe: usage and the knowledge gaps and challenges to wider adoption. Forestry 95 (1), 1–12. https://doi.org/10.1093/forestry/cpab038.

Mehtatalo, L., de-Miguel, S., Gregoire, T.G., 2015. Modeling height-diameter curves for prediction. Can. J. For. Res. 45 (7), 826–837. https://doi.org/10.1139/cjfr-2015-0054.

Mellander, P.-E., Löfvenius, M.O., Laudon, H., 2007. Climate change impact on snow and soil temperature in boreal Scots pine stands. Clim. Change 85, 179–193. https://doi.org/10.1007/s10584-007-9254-3.

Nabuurs, G.-J., Lindner, M., Verkerk, P.J., Gunia, K., Deda, P., Michalak, R., Grassi, G., 2013. First signs of carbon sink saturation in European forest biomass. Nat. Clim. Change 3 (9), 792–796. https://doi.org/10.1038/nclimate1853.

Nakagawa, S., Schielzeth, H., 2013. A general and simple method for obtaining R2 from generalized linear mixed-effects models. Methods Ecol. Evolution 4 (2), 133–142. https://doi.org/10.1111/j.2041-210x.2012.00261.x.

Ni, W., Woodcock, C.E., 2000. Effect of canopy structure and the presence of snow on the albedo of boreal conifer forests. J. Geophys. Res. 105 (D9), 11879–11888. https://doi.org/10.1029/1999JD901158.

O'Halloran, T.L., Law, B.E., Goulden, M.L., Wang, Z., Barr, J.G., Schaaf, C., Brown, M., Fuentes, J.D., Göckede, M., Black, A., Engel, V., 2012. Radiative forcing of natural forest disturbances. Glob. Change Biol. 18 (2), 555–565. https://doi.org/10.1111/j.1365-2486.2011.02577.x.

O'Halloran, T.L., Acker, S.A., Joerger, V.M., Kertis, J., Law, B.E., 2014. Postfire influences of snag attrition on albedo and radiative forcing. Geophys. Res. Lett. 41 (24), 9135–9142. https://doi.org/10.1002/2014GL062024.

Patterson, H.D., Thompson, R., 1971. Recovery of inter-block information when block sizes are unequal. Biometrika 58, 545–554. https://doi.org/10.1093/biomet/58.3.545.

Pohjanmies, T., Triviño, M., Le Tortorec, E., Mazziotta, A., Snäll, T., Mönkkönen, M., 2017. Impacts of forestry on boreal forests: an ecosystem services perspective. Ambio 46, 743–755. https://doi.org/10.1007/s13280-017-0919-5.

Pommerening, A., Murphy, S., 2004. A review of the history, definitions and methods of continuous cover forestry with special attention to afforestation and restocking. Forestry 77 (1), 27–44. https://doi.org/10.1093/forestry/77.1.27.

Potter, S., Solvik, K., Erb, A., Goetz, S.J., Johnstone, J.F., Mack, M.C., Randerson, J.T., Roman, M.O., Schaaf, C.L., Turetsky, M.R., Veraverbeke, S., Walker, X.J., Wang, Z., Massey, R., Rogersm, B.M., 2019. Climate change decreases the cooling effect from postfire albedo in boreal North America. Glob. Change Biol. 26 (3), 1592–1607. https://doi.org/10.1111/gcb.14888.

Ramtvedt, E.N., Næsset, E., 2023. A simple slope correction of horizontally measured albedo in sloping terrain. Agric. For. Meteorol. 339, 109547. https://doi.org/10.1016/j.agrformet.2023.109547.

Ramtvedt, E.N., Ørka, H.O., Bollandsås, O.M., Næsset, E., Gobakken, T., 2024. Effect of albedo footprint size on relationships between measured albedo and forest attributes for small forest plots. Remote Sens. 16 (16), 3085. https://doi.org/10.3390/rs16163085.

Randerson, J.T., Liu, H., Flanner, M.G., Chambers, S.D., Jin, Y., Hess, P.G., Pfister, G., Mack, M.C., Treseder, K.K., Welp, L.R., Chapin, F.S., Harden, J.W., Goulden, K.L., Lyons, E., Neff, J.C., Schuur, E.A.G., Zender, C.S., 2006. The impact of boreal forest fire on climate warming. Science 314 (5802), 1130–1132. https://doi.org/10.1126/science.1132075.

Rautiainen, M., Stenberg, P., 2005. Application of photon recollision probability in coniferous canopy reflectance simulations. Remote Sens. Environ. 96 (1), 98–107. https://doi.org/10.1016/j.rse.2005.02.009.

Rautiainen, M., Stenberg, P., Mõttus, M., Manninen, T., 2011. Radiative transfer simulations link boreal forest structure and shortwave albedo. Boreal Environ. Res. 16, 91–100.

R Core Team, 2024. R: a language and environment for statistcal computing. Available online. https://www.r-project.org/.

Roberge, J.-M., Laudon, H., Björkman, C., Ranius, T., Sandström, C., Felton, A., Sténs, A., Granström, A., Widemo, F., Bergh, J., Sonesson, J., Stenlid, J., Lundmark, T., 2016. Socio-ecological implications of modifying rotation lengths in forestry. Ambio 45, 109–123. https://doi.org/10.1007/s13280-015-0747-4.

Rogers, B.M., Soja, A.J., Goulden, M.L., Randerson, J.T., 2015. Influence of tree species on continental differences in boreal fires and climate feedbacks. Nat. Geosci. 8 (3), 228–234. https://doi.org/10.1038/ngeo2352.

Satterthwaite, F.E., 1941. Synthesis of variance. Psychometrika 6, 309–316.

Skakun, S., Wevers, J., Brockmann, C., Doxani, G., Aleksandrov, M., Batic, M., Framtz, D., Gascon, F., Gómez-Chova, L., Hagolle, O., López-Puigdollers, D., Louis, J., Lubej, M., Mateo-García, G., Osman, J., Peressutti, D., Pflug, B., Puc, J., Richter, R., Roger, J.-C., Scaramuzza, P., Vermote, E., Vesel, N., Zupanc, A., Žust, L., 2022. Cloud mask intercomparison eXercise (CMIX): an evaluation of cloud masking algorithms for Landsat 8 and Sentinel-2. Remote Sens. Environ. 274, 112990. https://doi.org/10.1016/j.rse.2022.112990.

Stokland, J.N., 2021. Volume increment and carbon dynamics in boreal forest when extending the rotation length towards biologically old stands. For. Ecol. Manag. 488, 119017. https://doi.org/10.1016/j.foreco.2021.119017.

Stuenzi, S.M., Schaepman-Strub, G., 2020. Vegetation trajectories and shortwave radiative forcing following boreal forest disturbance in eastern Siberia. J. Geophys. Res. 125 (6). https://doi.org/10.1029/2019JG005395 e2019JG005395.

Tahir, Z.R., Amjad, M., Asim, M., Azhar, M., Farooq, M., Ali, M.J., Ahmad, S.U., Amjad, G.M., Hussain, A., 2021. Improving the accuracy of solar radiation estimation from reanalysis datasets using surface measurements. Sustain. Energy Technol. Assess. 47, 101485. https://doi.org/10.1016/j.seta.2021.101485.

Tang, J., Luyssaert, S., Richardson, A.D., Kutsch, W., Janssens, I.A., 2014. Steeper declines in forest photosynthesis than respiration explain age-driven decreases in forest growth. PNAS 111 (24), 8856–8860. https://doi.org/10.1073/pnas.1320761111.

Wang, Z., Schaaf, C., Lattanzio, A., Carrer, D., Grant, I., Román, M., Camacho, F., Yu, Y., Sánchez-Zapero, J., Nickeson, J., 2019. Global surface albedo product validation best practices protocol. Version 1.0. Good Practices for Satellite-Derived Land Product Validation 45.

Webster, C., Jonas, T., 2018. Influence of canopy shading and snow coverage on effective albedo in a snow-dominated evergreen needleleaf forest. Remote Sens. Environ. 214, 48–58. https://doi.org/10.1016/j.rse.2018.05.023.

Wheeler, B., Torchiano, M., Torchiano, M.M., 2022. Package 'lmperm'. R package version 1 (1–2).

Wright, N., Duncan, J.M., Callow, J.N., Thompson, S.E., George, R.J., 2024. CloudS2Mask: a novel deep learning approach for improved cloud and cloud shadow masking in Sentinel-2 imagery. Remote Sens. Environ. 306, 114122. https://doi.org/10.1016/j.rse.2024.114122.